Simultaneous estimation of secular and episodic crustal motion via geodetic observations

C. Mitsakaki, A. Mimidou

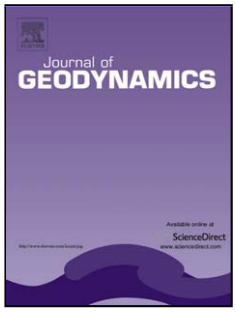

Title: Simultaneous estimation of secular and episodic crustal motion via geodetic observations

Authors: C. Mitsakaki, A. Mimidou

PII: S0264-3707(09)00112-4
DOI: doi:10.1016/j.jog.2009.10.001
Reference: GEOD 939

To appear in: *Journal of Geodynamics*

Received date: 26-11-2008
Revised date: 29-6-2009
Accepted date: 6-10-2009

Please cite this article as: Mitsakaki, C., Mimidou, A., Simultaneous estimation of secular and episodic crustal motion via geodetic observations, *Journal of Geodynamics* (2008), doi:10.1016/j.jog.2009.10.001

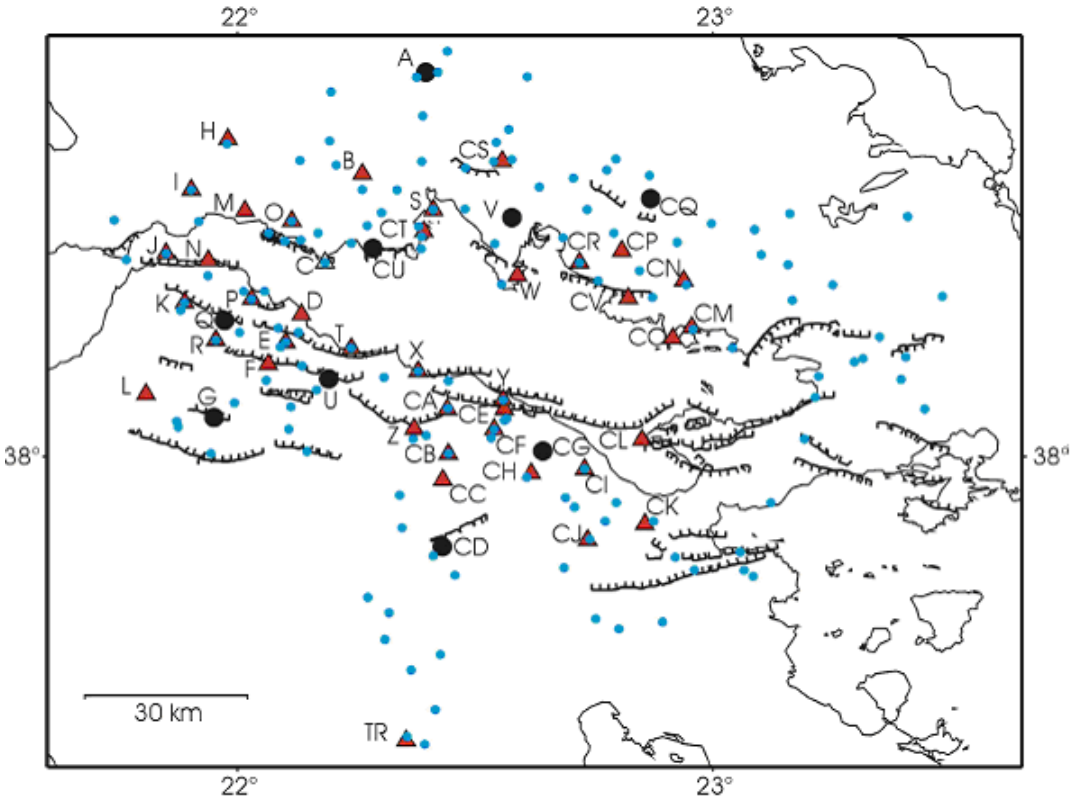

Figure 1 Positions of the gulf of Corinth GPS network points: red triangles, blue dots and black dots correspond respectively to the 1st order, 2nd order points (also old Hellenic triangulation network points) and to the ones common with the Central Greece network (another series of GPS campaigns in Greece). Dented segments show the localisation of the main active faults in the area. From (*Briole et al., 2002*).

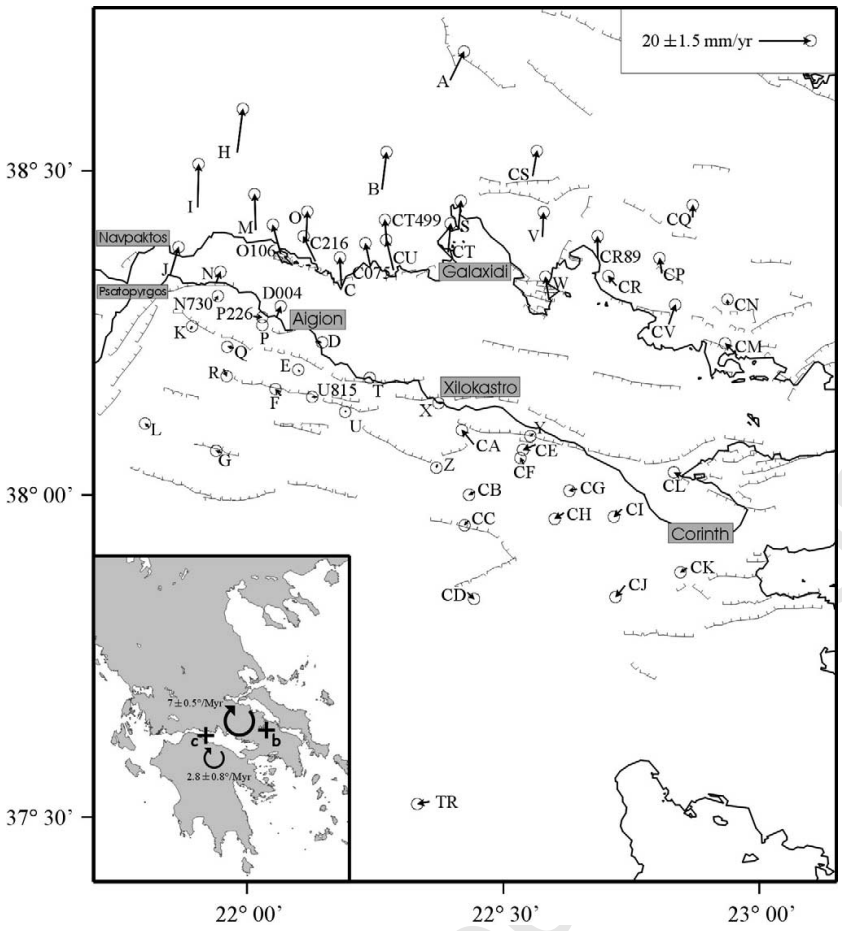

Figure 2 Smoothed velocity field (Peloponnesus fixed) from GPS observations between 1990 and 2000. The pole of rotation of the Central Greece block with respect to 'fixed Europe' is shown in inset. Its coordinates and rotation rate are given in Table 3 of Avallone et al., (*2004*).

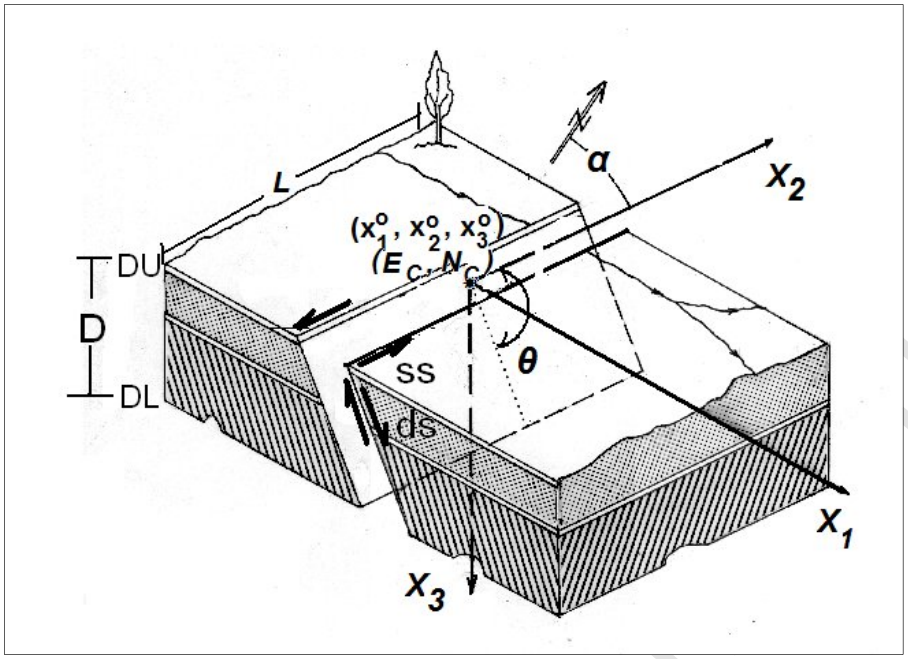

Figure 3 Dislocation model and fault geometry in a local three-dimensional Cartesian system (***x1, x2, x3***) with origin the centre of the fault trace at the earth's surface (x_1^o, x_2^o, x_3^o). (***EC, NC***) the reference system projection coordinates of the origin.

ss, ds Strike and dip slip of the dislocation parallelogram

α strike (azimuth) of the fault trace

θ dip angle

L fault length

D fault slab depth (DU: top, DL: bottom, D = DU-DL)

1992 and 1995 Earthquakes								
Date	**Ms**	**Mo** *(Nm)*	**Lat** *degrees*	**Long** *degrees*	**Length** *(km)*	**Strike** *degrees*	**Dip** *degrees*	**Top/Bottom** *(km)*
18/11/1992	5.9	0.5×10^{18}	38.30	22.45	14	270	30	5.2/9.7
15/06/1995	6.2	3.9×10^{18}	38.36	22.20	15	277	35	4.5/9.7

Table 2 Parameters for the offshore faults of the 1992 and 1995 earthquakes. The parameters are: **Ms** the magnitude of the event, **Mo** the seismic moment, **Lat** and **Long** the geodetic coordinates of the fault's center, **Length** the length of fault, **Strike** the fault's azimuth, **Dip** the fault's dipping angle and **Top/Bottom** the upper and lower depth of the fault (*Briole et al., 1993*), (*Bernard et al., 1997*), (*Avallone et al., 2004*)

		This work		
	Secular rate parameters	***All Epochs (1990-2001)*** *(3 fault segments for the episodic motion)*	***Epochs 1990-1997.8*** *(3 fault segments for the episodic motion)*	***Smoothed Data***
North block	$\dot{d}_E$ (mm/yr)	-2±1	-3±2	0±1
	$\dot{d}_N$ (mm/yr)	5±2	8±2	8±1
	$\dot{\rho}$ (μstr/yr)	.12±.02	.11±.03	.11±.03
	$\dot{\omega}$ (μstr/yr)	.08±.02	.11±.03	.10±.03
	$\dot{\gamma}$ (μstr/yr)	.30±.02	.22±.03	.22±.03
	A (degrees)	*17°.2*	*17°.1*	*13°.6*
	$\dot{e}_{max}$ (μstr/yr)	.25±.03	.22±.04	.21±.04
	$\dot{e}_{min}$ (μstr/yr)	-.02±.02	-.00±.02	-.00±.02
South block	$\dot{d}_E$ (mm/yr)	-0±1	-1±1	-2±1
	$\dot{d}_N$ (mm/yr)	1±1	2±1	-1±1
	$\dot{\rho}$ (μstr/yr)	.02±.02	-.00±.02	.08±.02
	$\dot{\omega}$ (μstr/yr)	.02±.02	.03±.02	.01±.02
	$\dot{\gamma}$ (μstr/yr)	.14±.02	.10±.03	.21±.02
	A (degrees)	*16°.1*	*16°.9*	*5°.3*
	$\dot{e}_{max}$ (μstr/yr)	.10±.03	.04±.03	.18±.03
	$\dot{e}_{min}$ (μstr/yr)	-.05±.02	-.05±.02	-.03±.02
	$\hat{\sigma}_o$ (mm/yr)	±**22**	±**12**	±**3**

Table 3 Secular strain parameters for the two homogenously deforming blocks (North and South). At the same time three fault segments are considered for the episodic motion: a single segment model for the 1992 Galaxidi earthquake and a double one (the upper slab and a lower relaxation segment) for the 1995 Aigion event. A is the azimuth of maximum strain rate (semiaxis of the strain ellipse) e_{max}.

The last column is taken from previous work (*Agatza et al., 2003*), (*Avallone et al., 2004*). It represents the secular parameters estimated after the average co-seismic motion for the 1995 Aigion earthquake (considered as a single dislocation segment) is eliminated from the GPS data.

	Slip for the 1992 and 1995 Earthquakes							
Cases examined			**Length** *(km)*	**Dip** *degrees*	**Top/Bottom** *(km)*	**Strike slip** *(m)*	**Dip slip** *(m)*	$\hat{\sigma}_o$ * *(m)*
First case	this study	Only 1992 Galaxidi	14	30	5.2/9.7	.95 ± .06	.90 ± .08	±.02
	*Slip values from (Briole et al., 1993)***	Only 1992 Galaxidi	*14*	*30*	*5.2/9.7*	*Total slip 0.12m*		
Second case	this study	1992 Galaxidi	14	30	5.2/9.7	.92 ± .02	.93 ± .05	±.038 / ±.030
	this study	1995 Aigion (*single block*)	15	35	4.5/9.7	1.0 ±.03	1.0 ± .04	
Third case	this study	1992 Galaxidi	14	30	5.2/9.7	.95 ±.01	.91 ± .03	±.022 /±.012
	this study	1995 Aigion (*2 blocks*) *Upper block*	15	35	4.5/9.5	1.01 ± .02	1.0 ± .02	
	this study	1995 Aigion (*2 blocks*) *Lower block*	20	80	9.5/19.5	1.02 ±.01	.70 ±.025	
Fourth case	this study	1995 Aigion (*2 blocks*) *Upper block*	15	35	4.5/9.5	1.0 ± .02	1.0 ± .02	±.022 / ±.012
	this study	1995 Aigion (*2 blocks*) *Lower block*	20	80	9.5/19.5	1.04 ± .02	.68 ± .03	
	*Slip values from (Bernard et al., 1997) ***	Only 1995 Aigion *(Single block)*	*15*	*35*	*4.5/9.7*	*Total slip 0.87m*		

1

Table 4 Parameters chosen and slip results for the 1992 and 1995 earthquakes with the a posteriori variance factor $\hat{\sigma}_o$ of the model. *First case*: Only the 1992 event modelled; *second case*: the 1992 and 1995 earthquakes modelled as single blocks; *third case*: the 1992 as a single block and the 1995 as a two block dislocation; *fourth case*: only the 1995 event modelled as a two block dislocation.

* The first values for the a posteriori $\hat{\sigma}_o$ of the model refer to the case of using all available GPS data (1990-2001) and the second one when only data from the interval 1990-1997.8 have been used.

** The shadowed rows refer to results from previous studies (*Briole et al., 1993*), (*Bernard et al., 1997*) for comparison.

GPS Campaigns	1990	1991	1992	1993	1994	1995.5	1995.8	1997*	2001
First order points	7	23	9	43	16	23	51	12	35
Second order points	-	9	-	34	24	22	84	10	23

Table 1 Overview of the GPS campaigns for the Gulf of Corinth.
***** The data were acquired within the frame of a project in the vicinity of the Gulfs of Euboea and Corinth (*Agatza-Balodimou et al., 2003*).

Simultaneous estimation of secular and episodic crustal motion via geodetic observations

*** C. Mitsakaki, A. Mimidou**

Laboratory of Higher Geodesy, School of Rural and Surveying Engineering,
National Technical University of Athens, Athens, Greece

Abstract

Repeated high quality geodetic observations allow the estimation of the free surface velocity field for a region. Usually, a yearly secular rate is estimated, while the possible episodic motion (seismic slip) due to an earthquake is evaluated via inversion of the geodetic data. The episodic motion influence is subtracted from the total field. The actual region and the respective geodetic observations affected by the seismic event are often assessed by rather vague criteria.

This paper deals with an attempt to estimate simultaneously the secular and the episodic two–dimensional crustal motion for a region by means of repeated GPS observations of a geodetic network, carried out for a number of epochs.

The model is applied to the Gulf of Corinth available GPS data, spanning a time interval of more than a decade, and the results are discussed.

Keywords: GPS Positioning, Deformation Measurements, Dislocations, Corinth Rift

---

* Corresponding Author at: Laboratory of Higher Geodesy, School of Rural and Surveying Engineering, National Technical University of Athens,
9 H. Polytechniou Str., Zographou, 157 80 Athens, Greece
E-mail address: topocris@central.ntua.gr

1. Introduction

Tectonic movements in continental areas are driven by the complicated mechanical behaviour of the earth's crust. Repeated geodetic observations allow the estimation of the velocity field of the earth's free surface at discrete locations and for distances of many kilometres from the traces of active faults. Nowadays, in many cases, networks of GPS permanent stations provide practically continuous monitoring. Therefore, such observations permit an independent direct estimation of the deformation gradient tensor for a deforming area.

Greece, with the highest seismicity rate in Europe, belongs, mostly, to a continental region, with tectonics controlled by complicated mechanical behaviour. The most pronounced characteristic is the high extension rate over the Aegean Sea. Thus, the southwestern Aegean moves, relative to Eurasia, toward the SSW at about 30-40 mm/yr (*Nyst and Thatcher, 2004*). Normal faulting, organized into sub-parallel systems distributed over areas of tens or even hundred kilometres wide, is a feature often appearing in actively extending regions on the continents.

One of the most prominent and active features of such a system of faults is the rift along the Gulf of Corinth, with a large seismicity rate. It is an area of high seismic risk, since it is surrounded by several large, densely populated cities, among them Athens. Therefore extensive research work has been carried out for more than a decade.

The Gulf of Corinth is the most rapidly extending rift system in Greece with about 120km length and 30km width and a WNW-ESE trend. It is believed to be active at the present rates since the last 5Myrs (*Taymaz et al., 1991*), (*Armijo et al., 1996*). Most of the active surface normal faults are located on the south side of the gulf (North Peloponnesus) while some south-dipping faults appear on its northern side (Sterea Hellas) (*Armijo et al., 1996*). Present day extension rates, estimated from GPS observations, for the eastern part of the gulf are significantly lower (~ 5 - 6mm / yr) than the central-western ones (*Briole et al., 2000*), (*Clarke et al., 1997*). Medium size seismic events of the order of M_S ~ 5.5 - 6.5 are often the case.

Since 1990 the Higher Geodesy Laboratory of NTUA, participating in a European multi-disciplinary research program concerning the tectonic behaviour of the area, contributes in the acquisition and analysis of the geodetic data (Corinth Rift Laboratory). Between 1990 and 2001 eleven epochs of observations with GPS receivers were carried out on a network consisting of about 200 points, out of which 142 are pillars belonging to the Hellenic triangulation network (*Figures 1*and *2, Table 1*). Today, beyond these periodically observed points, five permanent GPS stations have been established in the area for continuous monitoring (*Briole et al., 2001*).

The key objective of this long-term project is to combine methods and data in order to estimate the seismic hazard in the region. Data both from the periodic reoccupation of the dense geodetic GPS network and the ones derived from the small permanent network may be used for this purpose. More explicitly, not only

the evaluation of the *inter-seismic strain rate* across the Gulf of Corinth but also the estimation of the geometric parameters (*co-seismic fault slip*) of the episodic motion associated with seismic events is sought after.

Often the rapture of the fault occurs at depth and no surface trace of the slip is visible. Thus, in order to evaluate episodic motion parameters using the surface velocity field derived from geodetic observations (today mostly GPS ones) one has to solve an inverse problem which has no unique solution. For medium size seismic events a typical procedure is a trial-and-error one, while observations and data from other disciplines (seismology, geology etc) provide constraints for the solution of the problem via a dislocation model (e. g., *Snay et al., 1983*; *Hudnut et al., 1996*).

Thus, geodetic network points with repeated observations (e.g., GPS) considered relatively close to the location of the earthquake and therefore probably affected by the co-seismic displacements are chosen. The coordinate time series of these are computed and examined in order to assess whether their positions are influenced from the event and to what extent. A dislocation model is chosen, with some of its parameters constrained by other than geodetic data (e.g., aftershock distribution at depth) and its displacement field on the earth's free surface is compared with the one available from the geodetic observations. The procedure is repeated until the estimated dislocation model parameters best fit the surface displacement field.

In the present work a two-dimensional model is described that solves for both the secular and some parameters of the episodic motion and accepts all available geodetic data (coordinate time series) as observations. Medium to large seismic

events affect the velocity field of broad areas. The radius of interference is represented by a constraint embedded in the computer programme and easily adapted to the size of the earthquake. The model is applied for the Galaxidi 1992 and Aigion 1995 earthquakes and the results are discussed.

2. The model

Until today, the common technique for deformation studies using geodetic observations is to carry out campaigns where discrete network points on the earth's surface are occupied repeatedly. Therefore, the data are sparse both spatially and temporally, and they should be homogenized by referring them to the same geodetic reference frame (e.g., ITRF2000) and epoch in order to be further used. Moreover, geodetic observations, like all types of observations have random errors, while they may be, also, contaminated by systematic errors (biases)[1] or gross errors (mistakes or outliers)[2]. Therefore, their reliability has to be statistically tested. The deformation model that is estimated by the geodetic observations has also to be tested for its congruency and its parameters for their statistical significance. Only the parameters found statistically significant should remain in the final expression of the model.

[1] *Systematic errors* may appear in observations when necessary reductions are omitted, or the influence from various sources (such as the ionosphere effects on GPS measurements) may be not properly modelled etc. They usually obey physical laws and in most cases may be modelled by mathematical expressions.

[2] *Outliers* are mistakes occurring by negligence. They are large in size and relatively easily detected.

So far, the geodetic GPS observations available in Greece, remain mostly sparse and thus, inadequate to discern a combination of parameters regarding the fault geometry. Thus, the detection of which fault is responsible for a seismic event, its geometry and location are information derived primarily from geological and seismotectonic observations. At present, the model described here solves only for the strike and dip slip components of the episodic motion of a seismic event that occurred during the time interval for which adequate GPS observations are available. The software uses as data the displacement at a given position if that location is within the specified radius of the centroid of the earthquake.

With respect to the secular motion the area is considered as consisting of a mosaic of blocks with borders active fault traces or lines that distinguish changes in the velocity field.

Since the accuracy of the vertical component determined from GPS observations is at least two to three times worse than the horizontal components the two-dimensional approach was chosen in this study. Thus, a two-dimensional model was developed that solves for both the secular and the two episodic motion parameters (strike and dip slip). Due to the average size of displacements, the infinitesimal elastic strain theory is followed for the secular motion without loss of the required precision. The data consists of the two-dimensional projection coordinates of the network point positions (***E, N***) for the various epochs of observations derived from the three-dimensional GPS (***X, Y, Z***) ones.

Software, already written and used in previous studies (e.g. *Agatza-Balodimou et al., 2003*), was modified in order to solve for the episodic motion parameters with their respective full covariance matrices so as to test their statistical significance. It should be mentioned that the displacement residuals may be statistically inspected for outliers at a certain confidence level. Suspect observations are signalled by the programme but their elimination depends on the software user. The software accepts data consisting of as many files as the available epochs of observations. Each file referring to epoch t_j contains the arrays of the projected plane coordinates derived at the respective epoch. Furthermore, the program allows for breaking up the region into several blocks. The solution of the parameters is carried out using simultaneously all the pertinent data files for each block and/or seismic event. The advantage of the program lies in its ability to utilize positional information *sparse both in space and time* and solve for the deformation rate inside each block as well as the episodic motion.

The map projection coordinates ($\boldsymbol{E_i, N_i}$) of a network point $\boldsymbol{i}$, belonging to the $\boldsymbol{k}$-th block, at observation epoch $\boldsymbol{t}^{\,j}$, are modelled as function of the following; its coordinates ($\boldsymbol{E^o, N^o}$) at reference epoch $\boldsymbol{t^o}$, the secular homogeneous infinitesimal strain rate and the contribution of the $\boldsymbol{m}$-th seismic event that occurred at $\boldsymbol{t^m}$ time (*Mitsakaki, 1987*):

$$\begin{bmatrix} E_i^j - E_i^0 \\ N_i^j - N_i^0 \end{bmatrix}_k = \begin{bmatrix} \dot{d}_E \\ \dot{d}_N \end{bmatrix}_k (t^j - t^0) + \begin{bmatrix} \dot{\rho} + \frac{\dot{\gamma}_1}{2} & \dot{\omega} + \frac{\dot{\gamma}_2}{2} \\ -(\dot{\omega} - \frac{\dot{\gamma}_2}{2}) & \dot{\rho} - \frac{\dot{\gamma}_1}{2} \end{bmatrix}_k \begin{bmatrix} E_i^j - \overline{E}_0 \\ N_i^j - \overline{N}_0 \end{bmatrix} (t^j - t^0) + \quad (1)$$

$$+ \sum_m r(t^j, t^m) \cdot R_a \cdot \left[F_m(E,N) - F_m^o(\overline{E}_0, \overline{N}_0) \right] \cdot \begin{bmatrix} ss_m \\ ds_m \end{bmatrix}$$

For the rigid body translation and the secular homogeneous infinitesimal strain rates (first two terms of formula 1) the variables are:

(E_i^j, N_i^j)	Easting and Northing of point ***i*** at observation epoch ***j***
(E_i^0, N_i^0)	Easting and Northing of point ***i*** at reference epoch t^o
$(\overline{E}_0, \overline{N}_0)$	Easting and Northing of the network reference point, considered stable both in space and time
$(E_i^j - \overline{E}_0), (N_i^j - \overline{N}_0)$	***i*** point position with respect the reference point $(\overline{E}_0, \overline{N}_0)$
$(\dot{d}_E, \dot{d}_N)$	rigid body translation rate components
$\dot{\gamma}_1, \dot{\gamma}_2$	shear strain rate components
$\dot{\omega}$	solid body rotation rate
$\dot{\rho}$	dilatation rate
(t^0, t^j)	reference epoch and observation epoch ***j***

Often, maximum and minimum strain rates (i.e. the axes of the strain rate ellipse) e_{max} and e_{min} are also used, as well as the total shear rate $\dot{\gamma} = (\dot{\gamma}_1^2 + \dot{\gamma}_2^2)^{1/2}$.

The last term in formula (*1*), expressed as a summation, refers to the episodic motion. The term describes the change in position (E_i^j, N_i^j) of the i-th point due to the slip components of the slipping fault (ss_m and ds_m: slips on the fault surface parallel and transverse to the fault strike respectively). This change takes place at the instant t^m of an earthquake occurring on the m-th parallelogram that represents the fault surface. The total effect on the position of each point is given by summing up all contributions from the m- parallelograms.

The dependence of the episodic motion on time is made obvious in the case of the *step function* $r(t^j, t^m)$ used in the model which is defined by the conditions (*Snay et al., 1983*):

$$\text{for } t^m < t^o \qquad r(t^j, t^m) = \begin{cases} -1 & t^j < t^m \\ 0 & t^j > t^m \end{cases}$$

$$\text{for } t^m > t^o \qquad r(t^j, t^m) = \begin{cases} 0 & t^j < t^m \\ 1 & t^j > t^m \end{cases} \qquad (2)$$

Conditions (*2*) consider that the slip on the m-th parallelogram occurs instantaneously at the instant t^m even though this may result in mistakenly assigning a post-seismic activity to the co-seismic phase. However, a more refined model that would attempt to distinguish between the phases of the seismic cycle (pro-, co- and post-seismic cycle) would require continuous monitoring observations, at several network points. This, until recently, was not easily realized in the case of the GPS networks and still remains a demanding and rather expensive approach.

The functions of the last term of expression (*1*) correlate the fault slips ss_m and ds_m with the displacements on the earth's free surface. Quite often the fault rupture due to an earthquake does not reach the surface. If the fault rectangle is buried, the upper edge of the parallelogram that simulates the fault surface is projected vertically until it meets the earth's surface. The middle of this line is regarded as the centre of the fault (x_1^0, x_2^0, x_3^0) defining the origin of a local three-dimensional right-handed Cartesian system (x_1, x_2, x_3). The axis x_1 coincides with the direction of the fault dip, while the axis x_2 is taken parallel with the fault strike (*Figure 3*).

The displacement, in map projection coordinates, of an arbitrary point (E_i^j, N_i^j) on the earth's surface due to the m-th parallelogram is analysed in two components. One is oriented parallel to the fault azimuth (*along strike*) $u_{1m}(E, N)$ and the other transversely to this $u_{2m}(E, N)$. Then, from dislocation theory there are functions $f_{im}(E, N)$ and $g_{im}(E, N)$ (with i =1, 2) such that:

$$\begin{bmatrix} u_{1m}(E,N) \\ u_{2m}(E,N) \end{bmatrix} = \begin{bmatrix} f_{1m}(E,N) & g_{1m}(E,N) \\ f_{2m}(E,N) & g_{2m}(E,N) \end{bmatrix} \cdot \begin{bmatrix} ss_m \\ ds_m \end{bmatrix} \qquad (3)$$

Functions f_{im} and g_{im} depend on the point's position. They, also, depend on the geometry, the position and the orientation of the parallelogram as well as the Poisson ratio v, which characterizes the elasticity of the earth's crust. In this model the Okada dislocation formulae are used (*Okada, 1985*).

Formulae (*3*) refer to the local three-dimensional system (x_1, x_2, x_3), with origin the centre of the fault trace at the free surface. The origin's coordinates in the map

projection reference system are E_C, N_C. This point is considered free of displacement.

For a point on the earth's surface, with map projection coordinates $(E\_, N\_)$ before the m-th earthquake, the relation that connects the two-dimensional geodetic reference system (E, N) with the arbitrary local reference system (x_1, x_2) is:

$$\begin{bmatrix} E\_ - E_C \\ N\_ - N_C \end{bmatrix} = \begin{bmatrix} \cos\alpha & \sin\alpha \\ -\sin\alpha & \cos\alpha \end{bmatrix} \cdot \begin{bmatrix} x_1 \\ x_2 \end{bmatrix} \quad (4)$$

where α is the fault azimuth (*strike*).

The contribution of the dislocation expressed in the local system (x_1, x_2) due to the m-th event is the vector (u_{1m}, u_{2m}). Then, directly after the earthquake, the new projection coordinates of the point (E_+, N_+) are expressed as:

$$\begin{bmatrix} E_+ - E_C \\ N_+ - N_C \end{bmatrix} = \begin{bmatrix} \cos\alpha & \sin\alpha \\ -\sin\alpha & \cos\alpha \end{bmatrix} \cdot \begin{bmatrix} x_1 + u_{1m} \\ x_2 + u_{2m} \end{bmatrix} \quad (5)$$

where the point (E_C, N_C) is considered as free from motion.

Combining expressions (*4*) and (*5*) the influence of the m-th dislocation on the map projection coordinates of the point is:

$$\begin{bmatrix} E_+ - E\_ \\ N_+ - N\_ \end{bmatrix} = \begin{bmatrix} \cos\alpha & \sin\alpha \\ -\sin\alpha & \cos\alpha \end{bmatrix} \cdot \begin{bmatrix} u_{1m} \\ u_{2m} \end{bmatrix} = R_a \cdot \begin{bmatrix} u_{1m} \\ u_{2m} \end{bmatrix} \quad (5')$$

The motion due to the earthquake at the network reference point $(\overline{E}_0, \overline{N}_0)$, with regard to the fault origin (E_C, N_C), may be expressed by the functions (u^o_{1m}, u^o_{2m}) according to (*5′*). When the motion of the arbitrary point $(E_i,$

N_i) is expressed with respect to the reference point $(\overline{E}_0, \overline{N}_0)$, which is now considered stable, (*5′*) becomes:

$$\begin{bmatrix} \Delta_m E \\ \Delta_m N \end{bmatrix} = \begin{bmatrix} E_+^o - E_-^o \\ N_+^o - N_-^o \end{bmatrix} = R_a \cdot \begin{bmatrix} u_{1m} - u_{1m}^o \\ u_{2m} - u_{2m}^o \end{bmatrix}$$

Here (E_-^o, N_-^o) and (E_+^o, N_+^o), the coordinates of ***i*** point before and after the earthquake respectively, refer to the reference point $(\overline{E}_0, \overline{N}_0)$.

The above expression may be written as:

$$\begin{bmatrix} \Delta_m E \\ \Delta_m N \end{bmatrix} = \begin{bmatrix} E_+^o - E_-^o \\ N_+^o - N_-^o \end{bmatrix} = R_a \cdot \left[F_m(E,N) - F_m^o(\overline{E}_o, \overline{N}_o) \right] \begin{bmatrix} ss_m \\ ds_m \end{bmatrix} \qquad (6)$$

From (*3*) it is obvious that: $F_m(E,N) = \begin{bmatrix} f_{1m}(E,N) & g_{1m}(E,N) \\ f_{2m}(E,N) & g_{2m}(E,N) \end{bmatrix}$

while the expression $F_m^o(\overline{E}_o, \overline{N}_o) = \begin{bmatrix} f_{1m}(\overline{E}_o, \overline{N}_o) & g_{1m}(\overline{E}_o, \overline{N}_o) \\ f_{2m}(\overline{E}_o, \overline{N}_o) & g_{2m}(\overline{E}_o, \overline{N}_o) \end{bmatrix}$

refers to the network reference point.

Finally, the formula (*1*) for each ***k*** -th block and all ***m*** seismic events may be generalized as:

$$\delta = \left[\dot{d}_k + \dot{E}_k \cdot \delta(\overline{E}_0, \overline{N}_0) \right] \cdot \delta t + \sum_m r(t^j, t^m) \cdot R_a \cdot \left[F_m(E,N) - F_m^o(\overline{E}_0, \overline{N}_0) \right] \cdot \begin{bmatrix} ss_m \\ ds_m \end{bmatrix} \qquad (7)$$

The variables in formula (7) are:

$$\boldsymbol{\delta} = \begin{bmatrix} E_i^j - E_i^0 \\ N_i^j - N_i^0 \end{bmatrix}_k, \quad \dot{\boldsymbol{d}}_k = \begin{bmatrix} \dot{d}_E \\ \dot{d}_N \end{bmatrix}_k, \quad \dot{\boldsymbol{E}}_k = \begin{bmatrix} \dot{\rho} + \frac{\dot{\gamma}_1}{2} & \dot{\omega} + \frac{\dot{\gamma}_2}{2} \\ -(\dot{\omega} - \frac{\dot{\gamma}_2}{2}) & \dot{\rho} - \frac{\dot{\gamma}_1}{2} \end{bmatrix}_k ,$$

$$\boldsymbol{\delta}(\bar{E}_0, \bar{N}_0) = \begin{bmatrix} E_i^j - \bar{E}_0 \\ N_i^j - \bar{N}_0 \end{bmatrix}$$

The method described here has similarities to block modelling (e.g., *McCaffrey, 2002*), although ours is a much simpler model. For the part of the surface velocities due to a locked fault (episodic motion) McCaffrey (2002) uses the same dislocation formulae (*Okada, 1985*). However, the approach in McCaffrey (2002) refers to block-bounding faults that follow the stick-slip model (aseismic steady state slip and slip 'deficit', as it is called in the locked phase). The present work is better suited for active faults, not of necessity bordering a block, that slip due to an earthquake.

In the present work, the secular motion is described by the infinitesimal strain rate inside each block. We preferred strain rate modelling, instead of the GPS velocity field, since the requirement for a strictly common spatio-temporal reference frame is not essential in our case. Part of the strain rate tensor is the solid body rotation rate of the block. This rotation rate may be transformed to an Euler rotation rate according to McCaffrey (2002).

Another difference lies in the data used in the present work. The data are positional information from several GPS campaigns, and the model solves for strain

rates and co-seismic slips (*formula 7*). The data in the block modelling approach is, usually, smoothed averaged velocities that rather lack the inconsistencies of real data. However, they still need to refer to the same geodetic reference frame and the same epoch (e.g., ITRF2005, epoch 2007.5) in order to be used as data for deformation analyses (*McCaffrey, 2002*), (*Nyst and Thatcher, 2004*).

3. Analysis

Since 1990 the Higher Geodesy Laboratory of the National Technical University of Athens participated in a European multi-disciplinary research programme for monitoring the tectonic behaviour of the Corinth rift region. A GPS network, part of a much larger network was established in Greece by several research teams (*Briole et al., 2000*). The network includes about 50 first order points (measured at least three times in a given campaign). In addition, about 150 second order points were observed one or two times during at least one campaign. It should be mentioned that approximately 140 of these GPS network points are pillars of the Hellenic triangulation network.

Eleven GPS campaigns were carried out from 1990 to 2001 (*Table 1*). Two of them (November 1992 and June 1995) took place after the M_S = 5.9, 18 November 1992, Galaxidi and the M_S = 6.2, 15 June 1995, Aigion earthquakes.

For all campaigns, IGS precise orbits and data from IGS stations were used to tie the network to ITRF2000. No ambiguity fixing was allowed for baselines longer than 100 km, in other words between points in the network and the IGS sites. The average percentage of ambiguities fixed in the network was ~ 85% (*Avallone et al., 2004*). Expected sources of errors in each campaign's final results are the centring of the antennas for the horizontal components, and the antenna heights and troposphere modelling for the vertical component (*Avallone et al., 2004*). So far, only horizontal solutions of the GPS data have been employed for the Gulf analyses; the same applies here. Time series of the map projection coordinates offer average uncertainty estimation of the order of a few $mmyr^{-1}$, which is a more realistic estimate than the uncertainties based on the GAMIT solutions (*Avallone et al., 2004*).

Previous extensive research work carried out for the Gulf of Corinth shows that the extension of the rift is localised along a narrow offshore zone of about 10km width. The extension rate, as derived from about 11 years of GPS observations is not uniform, with an average of 11mm/yr in the central part of the rift (largest rate of 16mm/yr close to Aigion town) and tapering off to 5-6mm/yr at the eastern edge of the gulf (*Avallone et al., 2004*), (*Agatza-Balodimou et al., 2003*), (*Briole et al., 2002*).

In view of these findings and in order to keep the model as simple as possible it was decided to consider the area of the gulf as consisting of two blocks, the north and south.

It is estimated that for the central part of the rift all recent large earthquakes (Eratine of Phokida, M_S = 6.3, 1965; Antikyra, M_S = 6.2, 1970; Galaxidi, M_S = 5.8, 1992, Aigion, M_S = 6.2, 1995) activated offshore faults with shallow north-dipping planes (*Baker et al., 1997*). In contrast the deformation pattern of the western part of the Corinth rift differs in that all active normal faults dip at large angles (50° to 60°) suggesting a probably significant structural change (*Bernard et al., 2006*).

Since the first GPS campaign took place in 1990, it was decided, at first, to investigate only the Aigion 1995 earthquake for the episodic motion. The event was large enough to affect the displacement field of a broad region and GPS data were available both before and after its occurrence.

The Galaxidi 1992 earthquake, an event of smaller size, took place in 1992. At the time, the GPS network was only partially established. Thus, the velocity field was poorly resolved. However, an attempt was made to include this event in the analysis.

The parameters for the two earthquakes taken from previous studies are presented in *Table 2* (*Bernard et al., 1997*), (*Briole et al., 1993*), (*Mitsakaki et al., 2006*).

Several tests were carried out with respect to the sensitivity of the model to various dislocation parameters. Thus, different depths and dip angles were used and the resulting strike and dip slips were compared. Usually, the model appeared to be insensitive to minor changes of the aforementioned parameters. Radical changes of depth and dip angles affected the model but also decreased the statistical reliability of the solution.

Secular motion parameters

The most characteristic cases for the secular motion parameters of the North and South blocks are depicted in *Table 3*. It should be mentioned here that the displacement residuals were statistically inspected for outliers at the 99% confidence level. The respective suspect observations were eliminated and the revised data set was used for a new solution. The last column (*Table 3*) is extracted from previous work (*Agatza-Balodimou et al., 2003*), (*Avallone et al., 2004*) and presented here for comparison. The effect of the average co-seismic motion for the 1995 event was estimated and eliminated from the velocity field (*Avallone et al., 2004*). Then the secular parameters were estimated (*Agatza-Balodimou et al., 2003*).

In the present work the secular parameters of the 1990-1997.8 dataset appear to be in better agreement with the smoothed data ones –at least for the north block. This may be due to the way the smoothed field was estimated by Avallone et al.

(2004). They used linear regression models making use of all the GPS time series (1990-2001). A co-seismic offset for 15 points, located close to the 1995 event's epicentre, was estimated from the regression models. This co-seismic effect was subtracted from the total field of the affected points. Then the velocities estimated from the regression models were considered as the smoothed secular velocity field. Since the north block GPS points were the ones mostly affected by the 1995 event, the removal of the co-seismic effect by Avallone et al. (2004) is probably the critical factor for the smoothing out of the remaining secular displacement field. This smoothed field was used in Agatza-Balodimou et al. (2003) but the two blocks were treated separately and the respective secular parameters were independently estimated.

In the present work not only the secular motion for the two blocks but also the episodic motion was estimated simultaneously. Therefore, the effect of the 1995 event's episodic motion was also relieved in our model, especially for the north block. Hence, the secular motion solution of Avallone et al. (2004) of the smoothed field for the north block is very similar to ours.

In contrast, the present solution for the south block is similar whether the 1990-1997.8 dataset or all data (1990 - 2001) are used (*Table 3*, 1st and 2nd column). These secular strain rates are quite lower compared to the ones estimated in the previous work (*Table 3*, last column) (*Agatza-Balodimou et al., 2003*; *Avallone et al., 2004*). It appears that the present model allows for some network points of the south block (located around the region of Aigion and close to the coast) to be partially influenced by the co-seismic effect of the 1995 earthquake. Therefore, a

lower residual secular displacement field for this block remains, providing smaller secular strain rates.

Episodic motion parameters

In all cases the geodetically derived co-seismic fault slip was significantly larger than the values derived in previous studies (*Table 4*). Several trials took place in order to estimate the model that better fitted the data. Global congruency testing for choosing the best fitting model for the Galaxidi and Aigion events was carried out for all cases. No weighting of the GPS data was considered; therefore the test statistic used was:

$$\frac{\boldsymbol{u}^T\boldsymbol{u}/\boldsymbol{n}-\boldsymbol{m}}{\boldsymbol{\sigma}_o^2}=\frac{\hat{\boldsymbol{\sigma}}_o^2}{\boldsymbol{\sigma}_o^2}\le \boldsymbol{F}_{(1-\alpha,r,\infty)}$$

In the formula $\boldsymbol{u}$ is the vector of the model residuals, $\boldsymbol{r}=\boldsymbol{n}-\boldsymbol{m}$ the degrees of freedom (with $\boldsymbol{n}$ the observations and $\boldsymbol{m}$ the parameters to be estimated), $\boldsymbol{\sigma}_o^2$ the apriori variance factor and $\boldsymbol{F}_{(1-\alpha,r,\infty)}$ the limit value of the Fischer distribution. The statistical significance of the model parameters was also tested using the test statistic $\frac{\hat{\boldsymbol{x}}_i}{\hat{\boldsymbol{\sigma}}_{\hat{\boldsymbol{x}}_i}}\le\sqrt{\boldsymbol{F}_{(1-\alpha_o,r,1)}}$. Here $\hat{\boldsymbol{\sigma}}_{\hat{\boldsymbol{x}}_i}$ is the standard error of the $\hat{\boldsymbol{x}}_i$ parameter and $\boldsymbol{r}$ is the degrees of freedom of the model.

For the 1992 Galaxidi event, GPS data from the period 1990-1994 were used. The estimated slip is quite larger (~120cm total slip) than the previously derived one of 12cm (*Table 4,* first case, 2nd row) (*Briole et al., 1993*), while the two slip

components are statistically significant at the 95% confidence level (*Table 4,* first case, 1st row). However, these high rates may not represent realistically the true motion. This discrepancy may be due to the fact that no full covariance matrices were used for weighting the geodetic coordinates in the deformation model. The use of the full variance - covariance matrix of the coordinates as the weight matrix for a least squares adjustment of a deformation model controls the statistical significance of all the parameters. This significance has to do not with their high value but their real contribution to the model (*Agatza-Balodimou* and *Mitsakaki, 1985*). Thus, high rates of deformation parameters may still be statistically insignificant if properly weighted.

Furthermore, Briole et al. (1993) used not only the relatively few GPS data available at the time (1990-1992) but also seismotectonic information to constrain some of the dislocation parameters. The present study used only data from the GPS campaigns. Thus, their dislocation positional parameters (*Table 1*) were chosen as known and only the strike and dip slips were estimated. It appears, though, that the geodetic data alone may not be sufficient to constrain the episodic motion for the Galaxidi event properly.

The slip for the 1995 earthquake (*Table 4,* 8th row) is also larger than the 87cm estimated by Bernard et al. (1997). However, a slip of this size is in accordance with the Harvard solution of Mo = 5.1×10^{18}Nm (*Bernard et al., 1997*). Alternatively, using the seismic moment (*Table 2*, 2nd row) given by Bernard et al. (1997), and a slightly lower rigidity of $\mu = 2.9 \times 10^{10}$Nm^{-2}, instead of $\mu = 3.39 \times 10^{10}$Nm^{-2} used in their study, the slip is again of the order of 1m. Besides, the

Bernard et al. (1997) solution was derived using not only the GPS data but also the InSAR images available for the region.

For a number of network points, the size of the remaining residuals, after the 1992 and 1995 earthquakes had been modelled, was of the order of several cm (*Table 4*, second case). These points were rather far away from the 1995 Aigion earthquake area. This behaviour indicated possible post-seismic relaxation for the 1995 event. In order to evaluate whether such an event took place, the 1995 Aigion earthquake was modelled as a two block dislocation model. The upper one describes the co-seismic episodic motion, as previously discussed. The deeper one, with the same position and strike angle as the upper one, deals with the post-seismic relaxation (*Table 4*, third and fourth case, 3rd and 2nd rows respectively) (*Ergintav et al., 2002*), (*Feigl* and *Thatcher, 2006*).

Global congruency testing indicated that the best fitting model for the Aigion event was the one with two blocks. The statistical significance of the model parameters was also tested. In all two-block trials the model parameters for the episodic motion were found significant at the 95% confidence level.

Finally, the two-block model for the Aigion 1995 earthquake (i.e., *Table 4,* third and fourth case, 3rd and 2nd rows respectively) was chosen as best fitting the data. The upper block has the geometry estimated from Bernard et al. (1997), with a total slip of 100 ± 12cm. The deeper block dips 80 degrees, extends from 9.5km to 20km depth and has a length of 20km. In this case the a posteriori $\hat{\sigma}_o$ of the deformation

model improved significantly (i.e., from ±0.038m to ±0.022m in the case of using all epochs).When data from the 1990-1997.8 interval were used the a posteriori $\hat{\sigma}_o$ was improved from ±0.030m to ±0.012m respectively.

A statistical value that merits some reflection is the a posteriori $\hat{\sigma}_o$ of the deformation model (*Tables 3* and *4*). The inclusion of more epochs results in increasing the number of observations which, in turn, raises the degrees of freedom. However, the aposteriori $\hat{\sigma}_o$ of the model shows higher values in this case. The network around the Gulf of Corinth was established in a piecewise manner and the network geometry (points observed) differed in each campaign. Therefore, the remaining undetected errors (systematic errors and/or outliers) affect differently the precision of the respective coordinates of each campaign. In other words, not all epochs of observations are of equivalent quality. Since the model used these coordinates as data the residuals of the model are influenced. More explicitly, using more epochs may increase the degrees of freedom but, also, adds to the size of the quadratic sum of the residuals. Hence, the larger values of the aposteriori $\hat{\sigma}_o$ for the model.

A last comment on the values of the aposteriori variance of the model; the aposteriori $\hat{\sigma}_o$ of the two-block model for the Aigion earthquake is clearly improved against the single block model. This is evident even in the case discussed previously, when data from all epochs were used (*Table 4*, last column, first values of $\hat{\sigma}_o$).

4. Conclusions

The model described in this paper appears to be able to estimate the parameters for both the secular and episodic motion for a number of blocks and seismic events. However, a displacement field with good temporal and spatial coverage is necessary.

A modification of the model to account for possible post-seismic relaxation may improve its sensitivity to better discern between the inter-seismic and post-seismic behaviour of the area under study. The implementation of any post-seismic relaxation model will, obviously, increase the number of unknown parameters. The complexity of such a model would need data from continuous GPS stations in order to better resolve the overall tectonic behaviour of an area.

Furthermore, a full three-dimensional model using the GPS coordinates (X, Y, Z) should be considered in order to describe more accurately the actual three-dimensional dislocation model.

Finally, a topic that merits investigation is whether full covariance matrices for the coordinates would provide better estimates for the reliability of the model and the statistical significance of its parameters.

Acknowledgments

The authors would like to thank Prof. M. Sakellariou for offering valuable advice. This work was supported by the Basic Research Programme Leykippos (2006-2008) of the National Technical University of Athens.

REFERENCES

Agatza-Balodimou A.M., Mitsakaki C., *Deformation Studies in the Mornos Dam Area (Greece)*. Survey Review, Vol. 28, No 217, (1985).

Agatza-Balodimou A.M., Avallone A., Briole P., Karamitsos S., Marinou A., Mitsakaki C., Papazissi K., Veis G. (2003). Deformation Studies in the Corinthian Gulf via Multi-epoch Analysis of Geodetic Data, *11th FIG Intern. Symp. On Deformation Measurements, 25-28 May, Santorini, Greece*.

Armijo R., Meyer B., King G., Rigo A., Papanastassiou D., (1996). Quaternary evolution of the Corinth Rift and its implications for the Late Cenozoic evolution of the Aegean, *Geophys. J. Int., 126***,** 11–53.

Avallone A., Briole P., Agatza-Balodimou A.M., H. Billiris, Charade O., Mitsakaki C., Nercessian A., Papazissi K., Paradissis D., Veis G. (2004) Analysis of eleven years of deformation measured by GPS in the Corinth Rift Laboratory area. *Comptes Rendues Geoscience, Special Issue on the Corinth Rift Laboratory, Vol.336, Fasc. 4-5,* pp.301-312.

Baker, C., Hatzfeld, D., Lyon-Caen, H., Papadimitriou, E., and Rigo, A., (1997). Earthquake mechanisms of the Adriatic Sea and Western Greece, *Geophys. J. Int., 131,* 559-594.

Bernard P., Briole P., Meyer B., Lyon-Caen H., Gomez J.M., Tiberi C., Berge C., Hatzfeld D., Lachet C., Lebrun B., Deschamps A., Courboulex F., Larroque C., Rigo A., Massonet D., Papadimitriou P., Kasaras J., Diagourtas D., Makropoulos K., Veis G., Papazissi K., Mitsakaki C., Karakostas V., Papadimitriou E., Papanastasiou D., (1997). The M_S=6.2, June 15, 1995 Aigion earthquake (Greece): Evidence for low angle normal faulting in the Corinth rift. *Journal of Seismology, No 1*, pp. 131-150.

Bernard P., Lyon-Caen H., Briole P., Deschamps A., Boudin F., Makropoulos K., Papadimitriou P., Lemeille F., Patau G., Billiris H., Paradissis D., Papazissi K., Castarède H., Charade O., Nercessian A., Avallone A., Pacchiani F., Zahradnik J., Sacks S., Linde A. (2006). Seismicity, deformation and seismic hazard in the western rift of Corinth:

New insights from the Corinth Rift Laboratory (CRL). *Tectonophysics* **426**, pp. 7–30.

Briole P., Deschamps A., Lyon-Caen H., Papazissi K. and Martinod J., (1993). The Itea (M ~ 5.9) Earthquake of November 18, 1992. - Characteristics of the Main Shock Inferred from Body Wave and Ground Displacement Analysis. *Proc. of the 2nd Congress of the Hellenic Geophysical Union, Florina, Greece, 5-7, May*, 297-308.

Briole P. Rigo A., Lyon-Caen H., Ruegg J.C., Papazissi K., Mitsakaki C., Agatza-Balodimou A.M., Veis G., Hatzfeld D., Deschamps A., (2000). Active Deformation of the Gulf of Korinthos, Greece: Results From Repeated GPS Surveys Between 1990 and 1995. *JGR, Solid Earth, Vol.105, No B11*, 25605-25625.

Briole, P.; Billiris, H.; Felekis, S.; Papazissi, K.; Paradissis, D.; Veis, G.; Avallone, A.; Charade, O.; Nercessian, A. (2001). The Gulf of Corinth CORSEIS" permanent GPS network: framework and perspectives. Presented.at *EGS XXVI General Assembly,* Nice, France, March 2001.

Briole P., Avallone A., Agatza-Balodimou A.M., Billiris H., Charade O., Lyon-Caen H., Mitsakaki C., Papazissi K., Paradissis D., Veis G., Karamanou A., Marinou A., (2002). A ten year analysis of deformation in the Corinthian Gulf via GPS and SAR Inteferometry. *11th General Assembly of the WEGENER Project, June 12-14, Athens, Greece*.

Clarke P.J., Davies R.R., England P.C., Parsons B.E., Billiris H., Paradissis D., Veis G., Denys P.H., Cross P.A., Ashkenazi V., Bingley R., (1997). Geodetic estimate of seismic hazard in the Gulf of Korinthos. *Geophysical Research Letters 24,* 1303-1306.

Ergintav S., Bürgmann McClusky R., S., Çakmak R., Reilinger R. E., Lenk O., Barka A., and Özener H. (2002) Post-seismic Deformation near the İzmit Earthquake (17 August 1999, *M* 7.5) Rupture Zone, *Bulletin of the Seismological Society of America*, Vol 92, pp. 194 - 207.

Feigl Kurt L., Thatcher Wayne, (2006). Geodetic observations of post-seismic transients in the context of the earthquake deformation cycle *Comptes Rendus Geoscience, Vol.338, Issues 14-15,* pp.1012-1028

Hudnut K. W., Shen Z., Murray M., McClusky S., King R., Herring T., Hager B., Feng Y., Fang P., Donnellan A. and Bock Y., (1996). Co-Seismic Displacements of the 1994 Northridge, California, Earthquake, *Bulletin of the Seismological Society of America volume **86**, No. **1B**, pp. S19-S36.*

McCaffrey R., (2002). Crustal Block Rotations and Plate Coupling, in *Plate Boundary Zones, AGU Geodynamic Series Vol. 30,* 425 p.

Mitsakaki C., (1987) A Method for Deformation Studies in Two Dimensions Using Geodetic Data, *Dr. of Engin. Thesis, School of Rural & Surveying Engineering, National Technical Univ. of Athens,* Greece, (In Greek).

Mitsakaki C., Papazissi K., Sakellariou M., Marinou A., Tsinas D. (2006) Coulomb Stress Changes in the Gulf of Corinth (Greece) for the 1992-1995 Period. *3rd Symposium on Geodesy for Geotechnical and Structural Engineering and 12th Symposium on Deformation Measurements, May 22 - 24, Baden, Austria.*

Nyst M., Thatcher W., (2004). New constraints on the active tectonic deformation of the Aegean*, J.G.R.., 109, B11406.*

Okada, Y., (1985) Surface deformation due to shear and tensile faults in a half-space, *Bull. Seismol. Soc.Am., 75*, 1135-1154.

Okada, Y., (1992) Internal deformation due to shear and tensile faults in a half-space, *Bull. Seismol. Soc.Am.*, *82*, 1018-1040.

Snay R.A., Cline M.W., Timmerman E.L. (1983). Regional deformation of the earth model for the San Diego region, California, *JGR, Vol.88, No B6,* pp. 5009-5024.

1 Taymaz T., Jackson J.A., McKenzie D.P. (1991). Active tectonics of the
2 north and central Aegean Sea, *Geophys. J. Int. 106*, 433– 490.
3